

1 **Design, construction and optimization of a synthetic RNA** 2 **polymerase operon in *Escherichia coli*.**

3 Joep Houkes¹, Lorenzo Olivi¹, Zacharie Paquet¹, Nico J. Claassens^{1,*}, John van der Oost^{1,*}

4 ¹Laboratory of Microbiology, Wageningen University and Research, Stippeneng 4, 6708 WE
5 Wageningen, The Netherlands.

6 * To whom correspondence should be addressed. Nico J. Claassens Tel: +31612880653, Email:
7 nico.claassens@wur.nl Correspondence may also be addressed to John van der Oost Tel: +31610785536, Email:
8 john.vanderoost@wur.nl

9 Present Address: Zacharie Paquet, Biological CBRN Defense Laboratory (DLD-Bio), Defense
10 Laboratories Department, Belgian Defense, Brussels, 1030, Belgium

11 **Keywords:** RNA polymerase; operon; adaptive laboratory evolution; synthetic genomics

12

13 **ABSTRACT**

14 Prokaryotic genes encoding functionally related proteins are often clustered in operons. The compact
15 structure of operons allows for co-transcription of the genes, and for co-translation of the polycistronic
16 messenger RNA to the corresponding proteins. This leads to reduced regulatory complexity and
17 enhanced gene expression efficiency, and as such to an overall metabolic benefit for the protein
18 production process in bacteria and archaea. Interestingly, the genes encoding the subunits of one of
19 the most conserved and ubiquitous protein complexes, the RNA polymerase, are not clustered in a
20 single operon. Rather, its genes are scattered in all known prokaryotic genomes, generally integrated
21 in different ribosomal operons. To analyze the impact of this genetic organization on the fitness of
22 *Escherichia coli*, we constructed a bacterial artificial chromosome harboring the genes encoding the
23 RNA polymerase complex in a single operon. Subsequent deletion of the native chromosomal genes
24 led to a reduced growth on minimal medium. However, by using adaptive laboratory evolution the
25 growth rate was restored to wild-type level. Hence, we show that a highly conserved genetic
26 organization of core genes in a bacterium can be reorganized by a combination of design,
27 construction and optimization, yielding a well-functioning synthetic genetic architecture.

28 **INTRODUCTION**

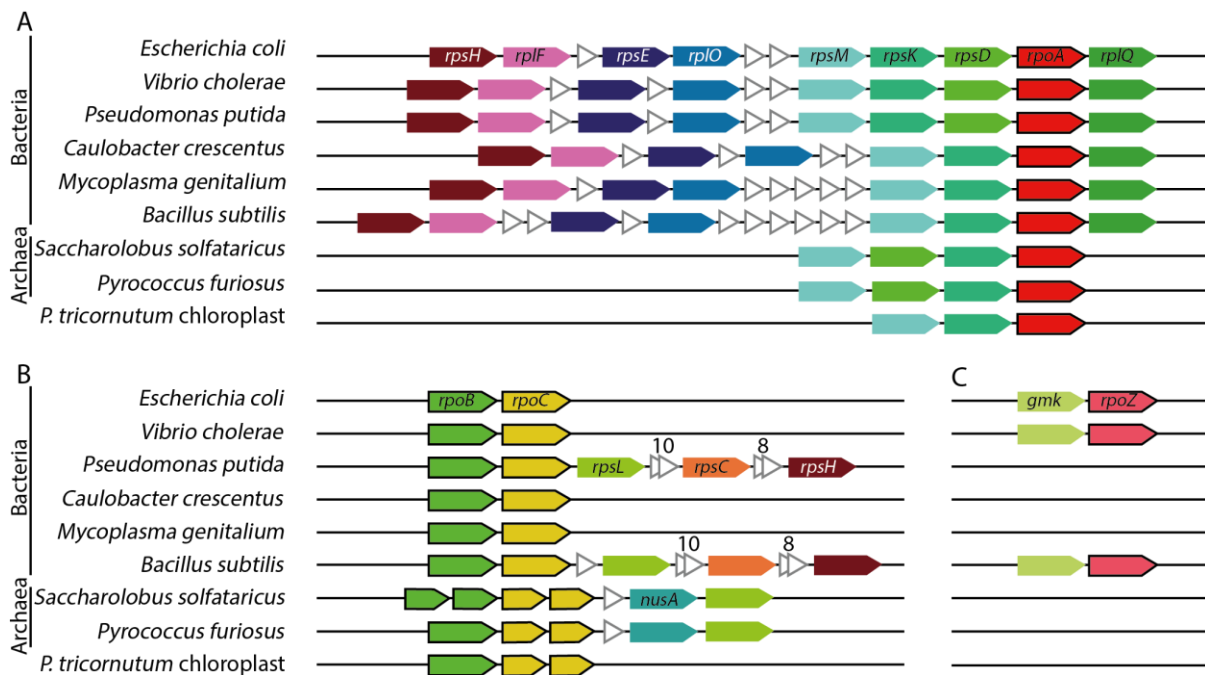
29 Operons were first described in the 1960s by Jacob and Monod as "a group of genes regulated by a
30 single operator" (1, 2). At present, operons are generally defined as clusters of genes that are co-
31 transcribed as a single polycistronic mRNA. As first observed in the lactose (*lac*) operon of *E.coli* (1,
32 2), subsequent experimental analyses of bacterial operons revealed that the clustered genes often
33 encode proteins (or RNAs) with related functions. Indeed, comparative genomics analyses
34 corroborated that operons are generally composed of functionally-related proteins ('guilt by
35 association'), such as enzymes of a metabolic pathway and subunits of a multi-protein complex (3, 4).

36 Ever since the discovery of the operon organization, the potential evolutionary forces that
37 drive operon formation have been discussed. Several hypotheses have been suggested to explain

38 how operons could potentially contribute to a selective advantage over individual genes: (i) operons
 39 contribute to reduction of genome size and to simplification of gene expression control (5), (ii) operons
 40 avoid energy loss through appropriate co-transcription and co-translation of functionally-related genes
 41 (6), and (iii) operons improve functional horizontal gene transfer (7–9).

42 In some metabolic pathways and protein complexes, uneven stoichiometries are required. In
 43 these cases it has been demonstrated that differential transcription occurs by using multiple
 44 promoters (4, 10), while differential translation of the cistrons within the operons is achieved in
 45 multiple ways. The rates of translation initiation can varied by tuning the strength of the Ribosome
 46 Binding Sites (RBS) and the mRNA secondary structure around the start codon, as well as by
 47 translation elongation, through modulating the codon bias (3, 11–13).

48 It is interesting to note that, despite being one of the most conserved protein complexes in the
 49 three domains of life, the genes coding for the subunits of the prokaryotic DNA-dependent RNA
 50 polymerase (RNAP) complex are not clustered in a single operon. At present, not a single prokaryotic
 51 genome is known in which the RNAP genes are organized as a single operon. Instead, the genes are
 52 spread throughout the genome at different loci. However, in bacteria, in archaea and even in the
 53 genomes of chloroplasts in photosynthetic eukaryotes (algae and plants), the RNAP genes are
 54 typically co-localized in distinct operons with ribosomal genes (Fig. 1).



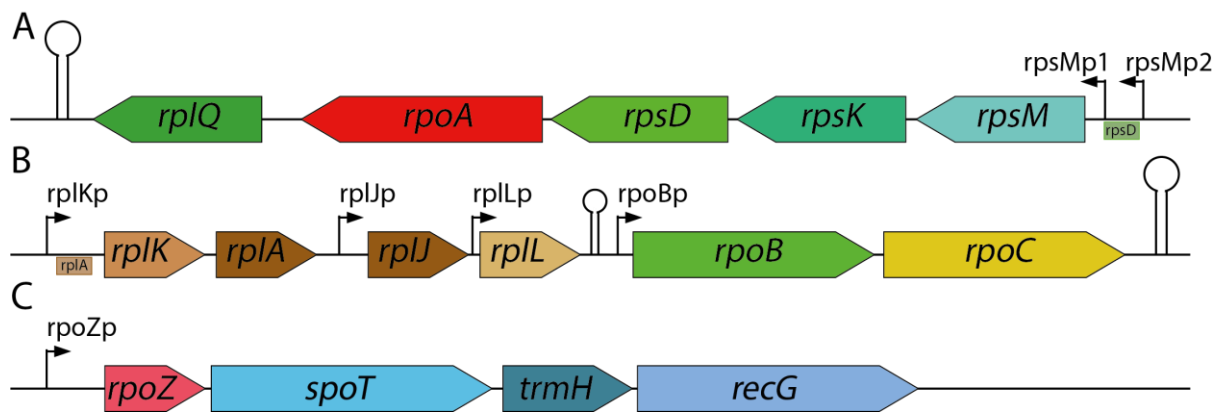
55
 56 **Figure 1. Syntheny of genes encoding core subunits of DNA-dependent RNA polymerase**
 57 **(RNAP).** (A) α subunit encoded by *rpoA* , (B) β and β' subunits encoded by *rpoB* and *rpoC* and (C) γ
 58 subunit encoded by *rpoZ* across selected bacterial and archaeal model species, as well as the
 59 chloroplast of the microalgae *Phaeodactylum tricornutum*. Same color genes indicate conserved
 60 clustering across species. Genes indicated by white triangles are not conserved. *Rps* and *rpl* genes
 61 encode ribosomal proteins (16S and 23S subunits, respectively), *nusA* encodes a transcription
 62 termination/anti-termination protein and *gmk* encodes a guanylate kinase. Figure generated with data
 63 from [STRING \(string-db.org\)](https://string-db.org).

64

65 The bacterial RNAP core complex consists of five subunits: two copies of the α subunits and
66 single copies of the β , β' and ω subunits (14). The *rpoA*-encoded α subunit dimer plays a key role in
67 assembly of the RNAP complex, acting as a scaffold for assembling the β and β' subunits (15).

68 Furthermore, the α subunit interacts with certain transcription factors to regulate transcription. The
69 *rpoA* gene of *E. coli* and many other bacteria is co-located in an operon harboring ribosomal genes
70 *rpsM*, *rpsK*, *rpsD* and *rplQ* (Fig. 1A, (16, 17).

71 The *rpoB* and *rpoC* genes encode the structurally related β and β' subunits, respectively, that
72 make up the hetero-dimeric core of the RNAP complex, of which the β' subunit harbors the catalytic
73 polymerase center (18, 19). Most likely the *rpoB* and *rpoC* genes are the result of a gene duplication
74 (18, 19). In line with this model, a single orthologous RNAP gene still exists in some phages, probably
75 encoding a homo-dimer (19). The bacterial *rpoB* and *rpoC* genes are always clustered, often
76 overlapping, and occasionally fused (20). In addition, a functional synthetic *rpoB-rpoC* fusion protein
77 has been reported (21). In several bacteria the *rpoB* and *rpoC* genes reside in an operon with the
78 ribosomal genes *rplK*, *rplA*, *rplJ* and *rplL* (Fig. 1B, 2B). In *E. coli*, this operon has a complex regulation:
79 involvement of four different promoters, regulation by multiple transcription factors and a
80 transcriptional attenuator terminating approximately 70% of transcription just upstream of *rpoB* (Fig.
81 2B) (22).



82

83 **Figure 2. Operons of the RNAP subunits in *E. coli*.** (A) operon harbouring the *rpoA* subunit of
84 RNAP, with the ribosomal genes *rpsM*, *rpsK*, *rpsD* and *rplQ* (16, 17). (B) operon harboring the *rpoB*
85 and *RpoC* subunits of RNAP, with the ribosomal genes *rplK*, *rplA*, *rplJ* and *rplL*. An attenuator
86 between *rplL* and *rpoB* halts approximately 70% of transcription (22). (C) operon harboring the *rpoZ*
87 subunit of RNAP, with *spoT*, involved in stringent stress responses (26–29), *trmH*, a tRNA
88 methyltransferase (25) and *recG* involved in DNA repair and DNA recombination (24).

89

90 The only non-essential subunit of the bacterial RNAP core is the ω subunit, which upon
91 knockout leads to growth retardation, but not to cell death (14, 23). The ω subunit is encoded by *rpoZ*,
92 which in *E. coli* resides in an operon with *trmH*, *recG* and *spoT* (Fig. 2C). TrmH is a tRNA
93 methyltransferase, and RecG is an ATP-dependent DNA helicase which plays a critical role in DNA
94 repair and DNA recombination (24, 25). SpoT is responsible for the synthesis and degradation of
95 ppGpp, the effector molecule for stringent response, which enables bacterial cells to react to stress

96 conditions by altering expression of many genes (26–29). Interestingly, the primary ppGpp binding
97 site of the *E. coli* RNAP is located at the interface of the β' and the ω -subunits. The ω subunit plays a
98 role in regulating ppGpp-dependent control of RNAP activity (30), and it has been reported to act as a
99 chaperone for the RNAP subunits (31). The ω subunit binds mainly to the β' subunit, close to the
100 active polymerase site, indicating a role in controlling the RNAP catalytic activity (18).

101 The RNAP $\alpha_2\beta\beta'\omega$ core forms a holoenzyme with a σ factor to initiate transcription. Bacteria
102 have several different σ factor, each of which is responsible for transcription of a specific subset of
103 genes (32). The housekeeping σ factor in *E. coli* is $\sigma70$, encoded by *rpoD* which controls a large
104 number of promoters, and regulates gene expression during 'normal' growth. Six additional σ factors
105 in *E. coli* each control the expression of a particular subset of genes, active during specific
106 environmental conditions (33). Regulation of σ factor expression is very complex, as they are very
107 condition-dependent, unlike the RNAP-core subunits, which are always present.

108 When comparing the amino acid sequences, the subunit composition, the overall structure,
109 the molecular mechanism and, to some extent, the genomic organization of RNAPs in all domains of
110 life, it becomes apparent they all derive from a common ancestor (34). Both the 13-subunit archaeal
111 and the 12-subunit eukaryotic RNAP complexes contain orthologues of the bacterial RNAP β -, β' -, α -
112 and ω -subunits. This reflects a common evolutionary history, in which the *rpoB/rpoC* gene pair
113 encodes the catalytic β/β' hetero-dimer of an ancient RNAP variant. At a later stage in the RNAP
114 evolution, the catalytic core was most likely supplemented with the *rpoA*-encoded α -subunit dimer,
115 and the *rpoZ*-encoded regulatory ω -subunit. The archaeal RNAP core resembles the bacterial RNAP
116 complex, with some additional genes encoding auxiliary subunits (34). The three basic eukaryotic
117 RNAPs (Pol I, II, III) and the 2 plant-specific RNAPs (Pol IV, V) are all derived from the archaeal
118 RNAP, each with specific sets of auxiliary subunits (34).

119 In this study, we set out to use a synthetic biology approach to test if this evolutionary-
120 conserved scattering of the RNAP genes can be reorganized into a single operon, and how such a
121 different architecture would impact cellular fitness. For this, we designed and constructed an operon
122 of the RNAP core genes in *E. coli*. This synthetic operon was introduced on a bacterial artificial
123 chromosome (BAC), and expressed in *E. coli*. Subsequently, native RNA polymerase genes on the *E.*
124 *coli* chromosome were knocked out, to assess the function of the RNA polymerase operon. This led to
125 a slightly lower growth rate on rich medium compared to wild-type *E. coli*, but, to almost complete loss
126 of growth on minimal medium. However, by adaptive laboratory evolution (ALE) on minimal medium,
127 we could restore growth and even improve the yield of the strain with the synthetic RNAP operon.
128 Overall, this study demonstrates that an evolutionary-conserved operon organization of a core protein
129 complex can be successfully reorganized, suggesting plasticity of genome organization and regulation.

130 MATERIAL AND METHODS

131 Strains and growth conditions

132 The *E. coli* DH10B strain (Invitrogen, suppl. table 2) was used for expression of the synthetic operon.
133 This strain was cultured at 37 °C in LB medium (10 g/L tryptone, 10 g/L NaCl, 5 g/L yeast extract),
134 2xYP medium (16 g/L peptone, 10 g/L yeast extract) or minimal M9+glucose medium (11.28 g/L 5x

135 M9 salts, 0.12 g/L MgSO₄, 5.5 mg/L CaCl₂, 3.6 g/l glucose supplemented with 0.1 mL 1000x trace
136 elements solution (50 g/L EDTA, 8.3 g/L FeCl₃·6H₂O, 0.84 g/L ZnCl₂, 0.13 g/L CuCl₂·2H₂O, 0.1 g/L
137 CoCl₂·2H₂O, 0.1 g/L H₃BO₃, 16 mg/L MnCl₂·4H₂O) and 0.5mM leucine) at 180 rpm or on LB-agar
138 plates containing 1.5% (w/v) agar (Oxoid) unless stated otherwise. The LB medium was
139 supplemented with different antibiotics (LB/Ab) when appropriate, to final concentrations of 20 µg/mL
140 kanamycin (Carl Roth) (Kan20), or 30 µg/mL chloramphenicol (Sigma Aldrich) (Cam30).

141 Yeast strain *S. cerevisiae* CEN.PK2-1D (*Euroscarf*, suppl. table 2) strain was used for
142 synthetic operon construction. This strain was cultured at 30°C in 10 mL YPD medium (20 g/L
143 peptone, 10 g/L yeast extract, 20 g/L glucose) or in SC medium (1.9 g/L nitrogen base without amino
144 acids, 5 g/L ammonium sulphate, 20 g/L glucose, 2g/L drop-out mix, appropriate auxotrophic marker
145 (76 mg/L uracil, 380 mg/L leucine, 76 mg/L histidine, 76 mg/L tryptophan)) in 50 mL tubes at 180 rpm.

146 **Preparation of electrocompetent cells**

147 *E. coli* cells were made electrocompetent by culturing at 37 °C in 2xYP (supplemented with 0.01 M L-
148 arabinose for recombination experiments), typically in 50 mL medium in 250 mL Erlenmeyer flasks, at
149 200 rpm until an OD_{600 nm} of 0.4 was reached. The cells were then cooled rapidly on ice, and
150 subsequently washed once with 1 culture volume of ice-cold ddH₂O and twice with 0.5 culture
151 volumes of ice-cold 10% glycerol. Finally, the cells were suspended in ice-cold 10% (vol/vol) glycerol
152 to a final volume of 200 µL for each 50 mL of initial culture volume.

153 Electroporation of 20 µL competent cells was performed in ice-cold 2 mm electroporation
154 cuvettes at 2500 V, 200 Ω and 25 µF (ECM 630 BTX). Immediately after electroporation, cell recovery
155 was performed in 1 mL LB medium at 37 °C, 750 rpm for 1 h when plasmids were transformed.
156 During recombination experiments, recovery was performed at 30 °C, 750 rpm for 2.5 h. After
157 recovery, the cells were plated on LB/Ab agar plates. Single colonies were picked and re-suspended
158 in 50 µL of ddH₂O for colony PCR and used to inoculate 10 mL of LB/Ab for overnight incubation and
159 subsequent isolation of plasmids, using GeneJET Plasmid MiniPrep Kit (Thermo Fisher Scientific).
160 The provided protocol was adjusted by initially centrifuging the cell cultures at 4700 rpm for 10 min,
161 and introducing of an incubation (2 min) at room temperature after addition of Elution Buffer or ddH₂O
162 (warmed to 70 °C).

163 Transformations of *S. cerevisiae* were performed by chemical transformation. Cells were
164 plated from glycerol stock on YPD, a single colony was picked for overnight culturing in YPD (typically
165 in 10 mL medium in 50 mL tubes, at 180 rpm). The culture was diluted to OD_{600nm} 0.4 in YPD and
166 incubated at 30°C, 200 rpm for 3 hours (typically in 50 mL medium in 250 mL Erlenmeyer flasks). The
167 cells were then washed with 0.5 culture volume of ddH₂O. Cells were resuspended in ddH₂O to a final
168 volume of 1 mL, aliquoted into 100 µL volumes and stored at 4°C for up to a week. To a 100 µL cell
169 suspension, 350 µL of a transformation mix (consisting of 240 µL PEG-3350, 36 µL 1 M LiOAc, 50 µL
170 2 mg/mL denatured salmon sperm DNA, and 34 µL of DNA mix containing 500 ng of DNA fragments
171 and 1 µg of backbone plasmid) was added. Next, the cells/transformation mix was heat-shocked at
172 42 °C for 40 min. The cells were resuspended in 1 mL YPD and 500 µL was used to inoculate 5 mL
173 YPD for overnight recovery, to boost the recombination efficiency. The remaining 500 µL was plated
174 on SC-agar plates with the appropriate auxotrophy markers. The success of the transformation was

175 assessed by colony PCR and single colonies were used to inoculate 10 mL SC with the appropriate
176 auxotrophy markers. For plasmid extraction, the cells were resuspended in 200 μ L GeneJET Plasmid
177 MiniPrep (ThermoFisher Scientific) resuspension buffer supplemented with 3 μ L 1000 U/mL Zymolase
178 (Amsbio) and incubated for 30 min at 37 °C to digest the cell walls. The rest of the extraction was
179 performed according to the MiniPrep protocol.

180 **Plasmid construction**

181 All PCR reactions for cloning purposes were performed using Q5® High Fidelity 2X Master Mix (New
182 England Biolabs). The reactions mixtures were prepared using 1 ng of template, 25 μ L Q5® High
183 Fidelity 2X Master Mix, primers to a final concentration of 500 nM, and ddH₂O to a final volume of 50
184 μ L (primers are listed in Suppl. table 4.). Amplification products were run on 0.7% agarose gels
185 stained with SYBR Safe DNA Gel Stain (Invitrogen). The bands of interest were then excised, and the
186 DNA purified using Zymoclean Gel Recovery kit (Zymo Research). Cloning was done using HiFi
187 assembly (New England Biolabs) according to manufacturer protocol. Overhangs for HiFi assembly
188 were added as 5' extensions of PCR-primers (list of plasmids in Suppl. table 3, list of primers in Suppl.
189 table 4).

190 **Preparation of knock-out strains**

191 Cells were transformed with a linear knock-out fragment with 50 bp recombination flanks harboring a
192 chloramphenicol resistance marker flanked by mutant *lox66* and *lox72* sites that upon recombination
193 are not recognized anymore by Cre recombinase (35). After recombination, single colonies were
194 picked, streaked on LB/Ab agar plates supplemented with isopropyl- β -D-thiogalactopyranoside (IPTG)
195 (Fisher Scientific, catalogue) to a final concentration of 0.5 mM, and then re-suspended in ddH₂O to
196 perform colony PCR to determine whether appropriate recombination occurred. IPTG-induced
197 expression of Cre recombinase from the BAC vector, generating mixed colonies with chloramphenicol
198 resistant (CmR) and sensitive (CmS) cells. These mixed colonies were re-streaked on LB/Ab plates.
199 Single colonies were picked from these plates and re-streaked on LB agar and in LB agar/Cam30.
200 CmS colonies were picked and re-suspended in ddH₂O to perform colony PCR, to confirm the
201 successful excision of the chloramphenicol resistance gene.

202 **Growth assays of knock-out strain and data analysis**

203 After knock-out was confirmed by colony PCR, growth assays were performed to assess growth rates
204 of the mutant strains. Precultures were prepared on LB for each strain and for wild-type DH10B.
205 Precultures were washed 3 times with ddH₂O and diluted to OD₆₀₀ 0.1. Next, 15 μ L of diluted
206 preculture of each strain and 135 μ L of LB or M9+Glucose was transferred in a 96-well plate. The
207 wells were covered with 50 μ L of mineral oil (Bio-Rad), to avoid evaporation during the experiment.
208 The plate was then incubated at 37 °C in a Biotek ELx800 absorbance microplate reader (Fisher
209 Scientific). The provided reader control software, Gen5, was used to set a measuring protocol
210 consisting of a cycle of 5 min of linear shaking followed by absorbance measurement at 600 nm, for at
211 least 24 h. The data were then exported to an Excel spreadsheet. An in-house MatLab script was
212 used to process the data, yielding strain-specific growth graphs and doubling times.

213 **sequencing and analysis**

214 For genomic sequencing analysis DNA was isolated and sequenced using Illumina NovaSeq paired
215 end 150bp. Mutation analysis was done using BreSeq(36) using the DH10B genome (NCBI ref.:
216 NC_010473.1) as reference. In addition, Genious Prime was used to map the sequencing results to a
217 DH10B reference genome and to validate the genomic knockouts of the four RNAP genes.

218 **RESULTS AND DISCUSSION**

219 **Designing and building a synthetic RNAP operon**

220 We rationally designed a synthetic RNAP operon in the order *rpoABCZ*. First, *rpoA* was introduced by
221 Gibson assembly on bacterial artificial chromosomes (BACs), controlled by a few different promoters
222 and RBS. One variant contained the native *rpoA* promoter, i.e. the *rpsMp2* promoter of the operon,
223 and the native *rpoA* RBS. In addition, *rpoA* was inserted downstream three constitutive promoters of
224 different strength (weak, moderate, strong) (37), that each were combined with one of 5 RBS in a
225 linearly increasing strength range (20, 40, 60, 80 and 98% of the predicted maximum strength), as
226 designed by EMOPEC (38). For each combination, the native *rpoA* gene on the *E. coli* chromosome
227 was knocked out, and a comparative growth assay on LB medium determined the best performing
228 combination: strong constitutive promoter and RBS80 (Suppl. table 1). Interestingly, knock-out of the
229 native *rpoA* gene was successful only for 7 out of 24 promoter-RBS combinations, strongly
230 suggesting that there is a certain range of *rpoA* expression levels that allows for *E. coli* survival. To
231 allow for easy addition and selection of subsequent subunits, we decided to move the marker directly
232 downstream of the operon. The *kanR* resistance marker was removed from the BAC-*rpoA* using the
233 λ -red system and *cre* recombinase. This created an addictive plasmid bale to be propagated because
234 of the presence of the essential *rpoA* gene. We then introduced *rpoB* with 6 different RBSs (native
235 and 5 synthetic variants) and a *kanR* gene directly downstream of *rpoA*. Deletion of chromosomal
236 *rpoB* gene and subsequent growth assays of the 6 RBS variants, showed that the native RBS
237 associated with *rpoB* on the BAC, resulted in the fastest growth. We aimed to continue this approach
238 for *rpoC* as well, but several attempts to introduce *rpoC* in the operon on the BAC were not successful.
239 To introduce *rpoC* we aimed to switch the antibiotic resistance gene in the BAC to *tetR*, to select for
240 BAC-*rpoABC* after transformation into the double knockout strain. Unexpectedly we did not obtain any
241 transformants harboring *rpoABC*. This prevented us from following the planned approach, to properly
242 introduce, delete and optimize expression for each RNAP gene one-by-one.

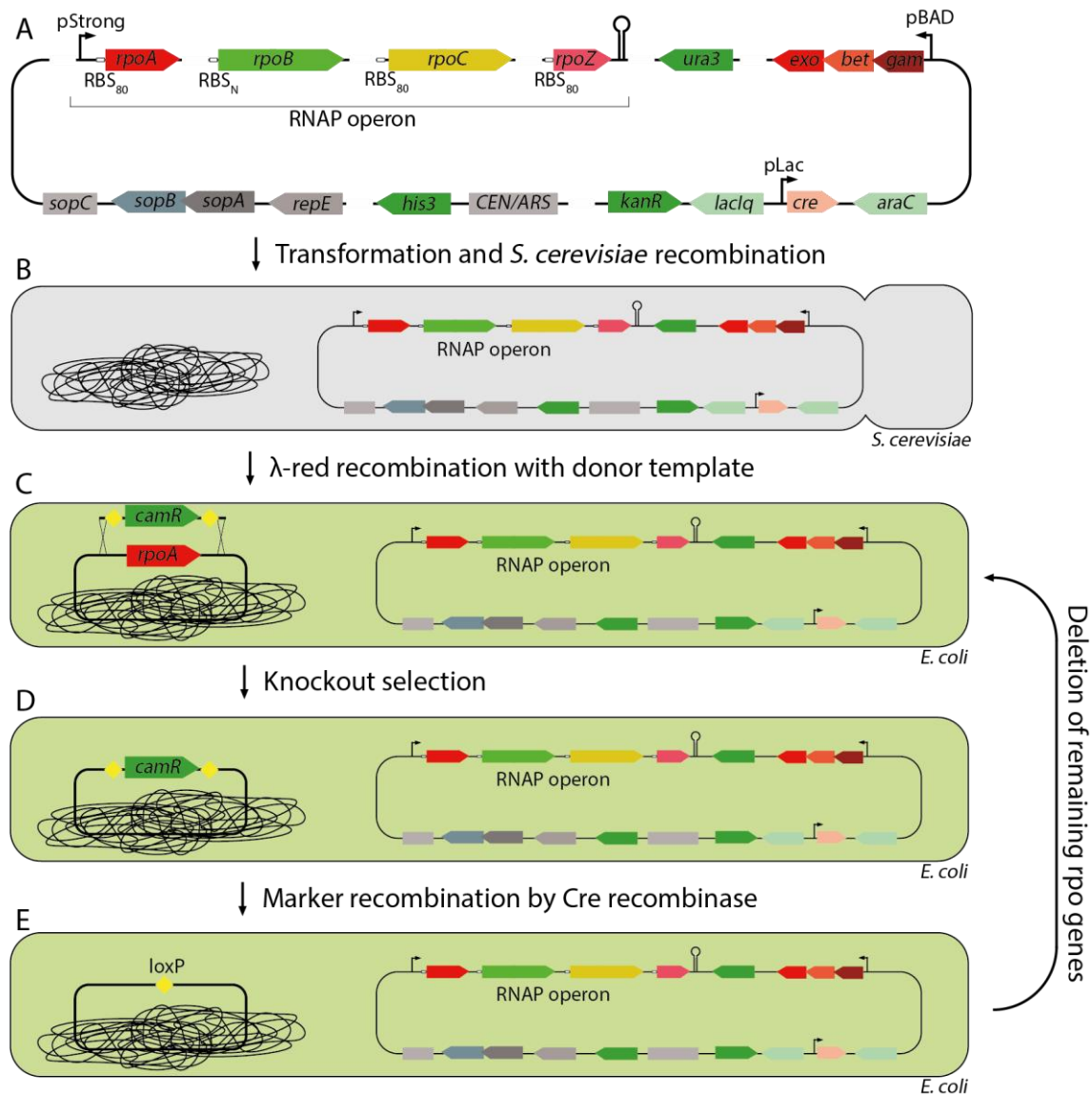
243 Therefore, an alternative approach was designed. As we could not continue with the one-by-
244 one optimization of the *rpo* genes, we decided to assemble the operon at once. Making a
245 combinatorial library of the synthetic *rpo* operon would lead to a large collection of *E. coli* strains from
246 which all genomic *rpo* genes would first need to be deleted and confirmed, leading to a major
247 experimental effort. Hence, we decided to use the previously identified well performing strong
248 promoter in combination with RBS80 for *rpoA*, and the native RBS variant for *rpoB*. In addition,
249 without prior knowledge, we tested the RBS80 variant upstream *rpoC* as well as upstream *rpoZ*.
250 Downstream *rpoZ*, we included an in-house designed synthetic terminator consisting of a stem-loop

251 and a T-stretch (5'-ccccgcttcggcggggtttttt) (Fig. 3). To efficiently assemble all these parts in the
252 relatively large BAC construct at once, we chose to further construct the BAC in *Saccharomyces*
253 *cerevisiae* because of its highly efficient recombination system. For that purpose, a BAC-yeast
254 artificial chromosome (BAC-YAC) shuttle vector was constructed. First, we PCR amplified the
255 bacterial replication system (*sopA*, *sopB*, *sopC* and *repE*) from a BAC (pBeloBAC11 (39)), as well as
256 the yeast centromere region from a YAC (pHLUM (40)) with a *his3* and a *ura3* selection marker.
257 Furthermore, the RNAP genes *rpoA*, *rpoB*, *rpoC* and *rpoZ* (and the aforementioned RBS variants)
258 were PCR-amplified from *E. coli* DH10B. To allow for eventually knocking out the native *rpo* genes,
259 the genes encoding the λ -red system (*gam*, *bet*, *exo*) and the Cre recombinase (*cre*) were PCR
260 amplified by using plasmid pSC020 (41) as a template. All PCR amplifications were carried out using
261 extended primers that generated specific 50 base pair overhangs to allow for efficient homologous
262 recombination in *S. cerevisiae*. Next, we transformed *S. cerevisiae* CEN.PK2-1D (histidine, leucine,
263 tryptophan, uracil auxotroph) with the 8 fragments as described above for homologous recombination
264 and selected for correct assemblies using medium lacking histidine and uracil (Fig. 3). The resulting
265 colonies were demonstrated by PCR to contain the designed BAC-YAC clone. Two of these colonies
266 were used for plasmid isolation and transformation into *E. coli* DH10B. From two *E. coli* DH10B
267 transformants, the sequence of the obtained BAC-YAC constructs was analyzed and confirmed to be
268 correct.

269 **Knockout strategy**

270 After transformation of *E. coli* DH10B with the BAC-YAC shuttle vector harboring the RNAP operon,
271 the native genes were knocked out using λ -red recombination (Fig. 3). For this, a repair template
272 containing a chloramphenicol resistance gene flanked by *lox66* and *lox72* sites was used (35). The
273 repair template was PCR-amplified using primers harboring overhangs homologous to the knockout
274 location. Using this approach, the chromosomal *rpoA*, *rpoB-rpoC* and *rpoZ* genes of the BAC-YAC-
275 containing *E. coli* strain were deleted consecutively (Fig. 3). The successful genomic deletions were
276 confirmed initially by PCR, and finally by genome sequencing. This confirmed that the synthetic
277 operon could fully replace the scattered genomic *rpo* genes.

278 To assess the growth of this newly created strain, named strain JH10B, growth assays were
279 performed on rich medium (LB) and minimal medium (M9+glucose), respectively (suppl. fig. 1). It was
280 found that on rich medium the growth rate of JH10B was slightly lower (reduced growth rate
281 approximately 7%) compared to growth of the wild-type *E. coli* DH10B. On minimal medium, however,
282 no growth was observed within the first two days for the engineered strain harboring the RNAP
283 operon (suppl. Fig. 1).



284

285 **Figure 3. Design and construction of RNAP operon on BAC-YAC and knockout of native genes.**

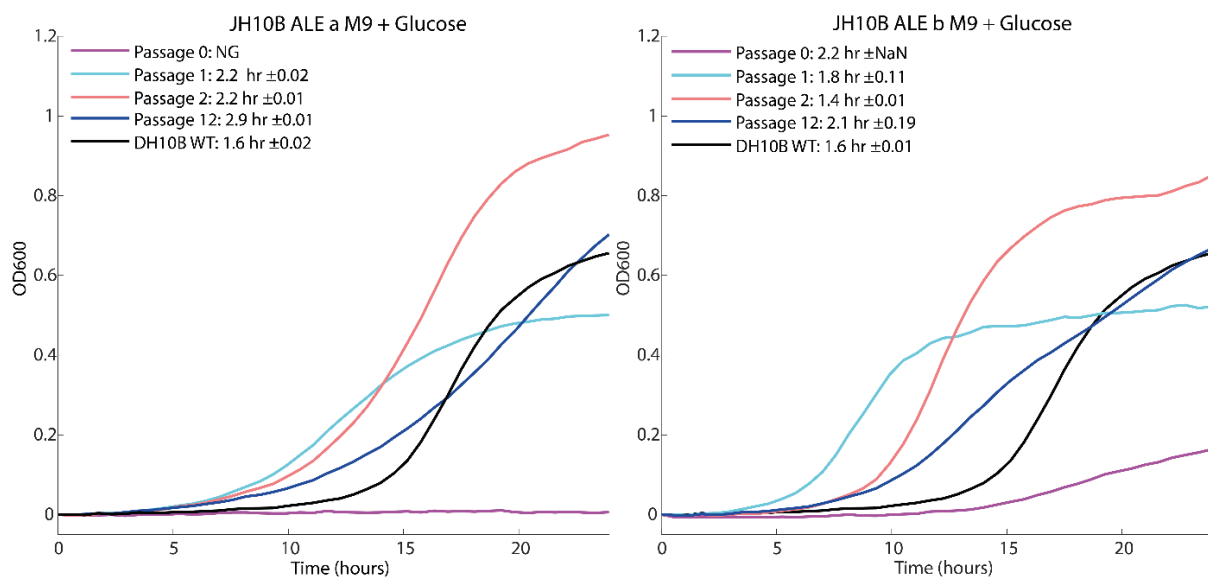
286 (A) Design of BAC and parts utilized for assembly. (B) Following this, yeast recombination, isolation
 287 and transformation into *E. coli* DH10B. (C) Knockouts are performed using λ-red recombination, (D)
 288 after which selection occurs using the antibiotic resistance marker. (E) Finally, the antibiotic
 289 resistance marker is recombined using Cre recombinase, leaving a dysfunctional *loxP* scar. Steps C-
 290 E are repeated for remaining *rpo* genes.

291

292 **Evolutionary optimization**

293 In an attempt to recover the ability of strain JH10B to grow on minimal medium, we decided to
 294 perform adaptive laboratory evolution (ALE) on M9+glucose. For this, two colonies (biological
 295 replicates a & b) were randomly selected and grown in 10 mL M9+glucose until the OD600 was at
 296 least 0.4. After this, 10 μL (0.1%) was transferred to a fresh tube with 10 mL M9+glucose, and after
 297 each passage a sample was taken for storage. After the first passage the obtained strain JH10B-ALE-
 298 1 already started growing on M9+glucose, and after 12 passages (strain JH10B-ALE-12) a plate

299 reader experiment was done to assess growth of selected generations of the adapted strains (JH10B-
300 ALE-1,-2,-3,-4,-8,-12) in minimal and rich medium, compared to the wild-type strain (Fig. 4, suppl. fig.
301 2). Although the lag-phase of the wild-type is shorter than the lag phases of the ALE strains, the
302 growth rate of the evolved strains is higher (up to 23%). Already after one round of ALE, the doubling
303 time of both biological ALE-1 replicates (strains JH10B-ALE-1a/b; 2.2/1.8 hrs respectively) was
304 comparable to the wild-type strain (1.6 hrs), whereas after the second round of ALE the evolved strain
305 (JH10B-ALE-2b) grows faster than the wild-type on M9+glucose medium (1.4 hrs). Additionally, the
306 yield (final OD600) of some of the evolved strains (JH10B-ALE3b; 1.39) are substantially higher
307 compared to the yield of the wild-type strain (0.66) (suppl. fig. 2). While this experiment enhanced the
308 growth rate of JH10B on M9+glucose, growth on LB did decrease (approximately 42% for JH10B-
309 ALEa and 35% for JH10B-ALEb) during the experiment (Suppl. fig. 3).



310

311 **Figure 4. Growth assays of *E. coli* strains harboring the RNAP operon after ALE on M9 medium**
312 with glucose. Representation of each line shown in figure legend. Doubling time and standard
313 deviation of 6 replicates are indicated.

314

315 **Genome sequencing and mutational analysis**

316 Whole-genome sequencing was performed on both biological replicates of the strains obtained after
317 one adaptation cycle (JH10B-ALE1a and JH10B-ALE1b), with the wild-type (passage 0) as control. In
318 total one unique mutation was found in *rpoB* in JH10B-ALE1a (T563P) and one unique mutation in
319 *rpoC* in JH10B-ALE1b (128LDMPL duplication), compared to the parental strain. Another mutation in
320 *rpoA* (Y68C) was found not only in both ALE1 replicates, but also in passage 0, before ALE (Table 1).
321 Sequencing results indicate that this mutation appeared either during PCR amplification or during
322 yeast recombination/replication of the fragment. Visual inspection of the crystal structure indicates
323 that the duplication in *rpoC* is located at the interface of the DNA strand. The mutation in *rpoA* in both
324 replicates localizes in a loop close to the binding site with the β and β' subunits.

325

326 **Table 1. mutations in *E. coli* strains harbouring RNAP operon after ALE experiment**

Gene	Passage 0	Passage 1	Passage 2	Mutation & function
Biological replicate a				
intergenic	A	A	G	Downstream of putative HNH nuclease <i>yajD</i>
<i>rpoA</i> (in operon)	A (WT=G)	A	A	Y68C
<i>rpoB</i> (in operon)	A	C	C	T563P substitution
Biological replicate b				
<i>yidZ</i>	T (WT=C)	T	T	R297W HTH-type transcriptional regulator Involved in anaerobic NO protection
<i>ilvE</i>	C	C	T	A259V Aminotransferase (leucine, isoleucine, valine, phenylalanine)
<i>lptF</i>	T	T	C	L311P translocation of LPS from the inner to the outer membrane
<i>rpoA</i> (in operon)	A (WT=G)	A	A	Y68C
<i>rpoC</i> (in operon)		TCGATAT GCCGCTGC	TCGATAT GCCGCTGC	Duplication of LDMPPL at position 128

327

328 Interestingly, but perhaps not surprisingly, during previously performed ALE experiments with
329 *E. coli*, mutations are frequently found in the genes encoding the RNAP subunits (42–47). In one of
330 these studies it has been concluded that mutations in the RNAP complex can generally satisfy
331 selection of enhanced growth rates under many conditions (47). Being the most central transcriptional
332 regulatory hub, many amino acid substitutions at relevant sites in the RNAP complex can potentially
333 lead to differences in the host's transcriptional profile (48, 49). In one study, 80% of *E. coli* MG1655
334 strains that were adapted to a minimal medium with glycerol as carbon source, appeared to harbor
335 mutations in the *rpoC* gene (46). These *rpoC* mutations appeared to lead to a 60% increase in growth
336 rate in glycerol minimal medium after reintroduction to MG1655 while simultaneously changing the
337 expression pattern of 900-1200 (20–27%) of its genes. At the time of writing, in ALEdb
338 (www.ALEdb.org), a web-based platform that reports on published ALE-acquired mutations for *E. coli*
339 contains 21738 unique mutations. Of these, 132 were found in *rpoB*, 109 in *rpoC* and 47 in *rpoA* and
340 none in *rpoZ*, for a total of 288 unique mutations, 1.32% of all unique mutations from the database,
341 while these genes make up 0.21% of the *e coli* genome(50). The mutation found in *rpoB* in this study
342 (T563P) has been found before during ALE on minimal medium, this mutation could confer rifampicin
343 resistance(47).

344 Although selection for enhanced growth under specific conditions very often leads to
345 mutations in RNAP genes, this often comes with a cost. While the fitness increases in the selected
346 environments, it decreases in different environments (46, 51, 52). In the present study, ALE on M9
347 glucose led to faster growth in this condition (Fig. 4), but to reduced growth on LB medium (suppl. fig.
348 3). The obtained amino acid substitutions can have different effects on the subunit, and on the RNAP
349 complex. Some studied mutations in *rpoC* have been shown to decrease open complex half-life (46,
350 53), which affects the transcription initiation and elongation activity (54). These studies also show that
351 down-regulated genes often have promoters with stress-related σ factors, whereas up-regulated
352 genes rather tend to have growth-related σ factors (53). It is not exactly known how mutations in
353 RNAP genes modulate the expression of genes that lead to certain phenotypes. However, the RNAP
354 complex can be regarded as the ultimate transcriptional regulator, allocating the cellular resources to
355 the specific molecular functions.

356 **Lessons for synthetic genome re-organization and modularization**

357 Based on the here presented successful transplantation of separate chromosomal genes to a fully
358 functional BAC-based RNAP operon, we conclude that, at least under the tested conditions, the
359 ubiquitous 'coupling' of the bacterial and archaeal RNA polymerase genes with the ribosomal genes is
360 not essential for life. This is an encouraging result for the design and construction of synthetic
361 genomes, based on partial rational combinations of components. Some attempts to construct
362 rearranged synthetic genomes have already been made, most notably in a minimized *Mycoplasma*
363 species JCVI-Syn3.0(55) and in *S. cerevisiae* (56). In *S. cerevisiae*, a core set of 13 glycolysis genes,
364 which in nature are scattered across the yeast chromosomes, were expressed from one chromosomal
365 locus using the native promoters, after which the native genes were deleted. This led to a strain which
366 was phenotypically similar to the wild-type strain. This demonstrated that co-localization of genes is
367 feasible even for a eukaryotic species with multiple chromosomes. In the prokaryotic minimal cell
368 JCVI-Syn3.0, genome reorganization towards clustering of functionally related genes was attempted
369 as well. First, genes were split in seven different categories for co-localization (e.g. DNA repair,
370 transcription, translation, glycolysis). Then the genome was split in eight segments, and for each
371 segment separately all genes belonging to one category were co-localized within this segment.
372 However, this meant that some original operon structures had to be rearranged. Hereto, a relatively
373 random approach was followed by which promoters/RBS were manually selected without any
374 optimization to regulate the reorganized genes. This highly randomized approach still led, maybe
375 surprisingly, to viable cells after modularization of one out of eight segments. However, the other
376 seven reorganized segments did not lead to viable cells. The latter result strongly suggests that a
377 rational approach should probably be combined with a random/combinatorial approach as described
378 in this study, to allow for selecting appropriate combinations of promoter and RBSs.

379 In conclusion, the current study reveals how modularization in bacteria can be performed via
380 a step-wise introduction of genes with synthetic control elements (promoters, RBSs) and subsequent
381 deletion of the native genes. This approach could be the basis to modularize larger parts of the
382 genome. After introduction of a synthetic gene or operon with a small library of synthetic promoters or
383 RBS, the native gene(s) can be deleted to identify viable clones, which could optionally be further

384 improved by ALE. This strategy will take relatively long, but could be speeded up lab-automation.
385 Eventually this may lead to a fully reorganized modular genome, that could be highly beneficial for
386 easy 'swapping' of modules when engineering cells towards desired applications.

387 **AVAILABILITY**

388 All data included in this study is available upon request by contact with the corresponding author.

389 **ACKNOWLEDGEMENT**

390 We thank dr. Sjoerd Creutzburg for supplying plasmid pSC020 and the synthetic terminator, and dr.
391 Arren Bar-Even for supplying the MatLab script for determining growth rates.

392

393 **FUNDING**

394 J.H., N.J.C., and J.v.d.O. acknowledge the support of the Netherlands Organization for Scientific
395 Research (NWO) via the Gravitation Project BaSyC (024.003.019) and Spinoza (SPI 93-537),
396 awarded to J.v.d.O. In addition, N.J.C. acknowledges support from his NWO Veni fellowship
397 (VI.Veni.192.156).

398 **CONFLICT OF INTEREST**

399 Authors state no conflict of interest.

400

401 **REFERENCES**

- 402 1. Fani,R., Brilli,M. and Liò,P. (2005) The Origin and Evolution of Operons: The Piecewise Building
403 of the Proteobacterial Histidine Operon. *J. Mol. Evol.*, 60, 378–390.
- 404 2. Jacob,F. and Monod,J. (1961) Genetic regulatory mechanisms in the synthesis of proteins. *J. Mol.*
405 *Biol.*, 3, 318–356.
- 406 3. Aravind,L. (2000) Guilt by Association: Contextual Information in Genome Analysis. *Genome*
407 *Res.*, 10, 1074–1077.
- 408 4. Huynen,M. (2000) Predicting Protein Function by Genomic Context: Quantitative Evaluation and
409 Qualitative Inferences. *Genome Res.*, 10, 1204–1210.
- 410 5. Nuñez,P.A., Romero,H., Farber,M.D. and Rocha,E.P.C. (2013) Natural Selection for Operons
411 Depends on Genome Size. *Genome Biol. Evol.*, 5, 2242–2254.
- 412 6. Sneppen,K., Pedersen,S., Krishna,S., Dodd,I. and Semsey,S. (2010) Economy of Operon
413 Formation: Cotranscription Minimizes Shortfall in Protein Complexes. *MBio*, 1.
- 414 7. Woese,C. (1998) The universal ancestor. *Proc. Natl. Acad. Sci.*, 95, 6854–6859.
- 415 8. Richard Dawkins (1976) *The Selfish Gene*.

- 416 9. Lawrence, J. (1999) Selfish operons: the evolutionary impact of gene clustering in prokaryotes
417 and eukaryotes. *Curr. Opin. Genet. Dev.*, 9, 642–648.
- 418 10. Wade, J.T., Roa, D.C., Grainger, D.C., Hurd, D., Busby, S.J.W., Struhl, K. and Nudler, E. (2006)
419 Extensive functional overlap between σ factors in *Escherichia coli*. *Nat. Struct. Mol. Biol.*, 13, 806–814.
- 420 11. Li, G.-W., Burkhardt, D., Gross, C. and Weissman, J.S. (2014) Quantifying Absolute Protein
421 Synthesis Rates Reveals Principles Underlying Allocation of Cellular Resources. *Cell*, 157, 624–635.
- 422 12. Quax, T.E.F., Wolf, Y.I., Koehorst, J.J., Wurtzel, O., van der Oost, R., Ran, W., Blombach, F.,
423 Makarova, K.S., Brouns, S.J.J., Forster, A.C., et al. (2013) Differential Translation Tunes Uneven
424 Production of Operon-Encoded Proteins. *Cell Rep.*, 4, 938–944.
- 425 13. Quax, T.E.F., Claassens, N.J., Söll, D. and van der Oost, J. (2015) Codon Bias as a Means to
426 Fine-Tune Gene Expression. *Mol. Cell*, 59, 149–161.
- 427 14. Burgess, R.R. (1969) Separation and Characterization of the Subunits of Ribonucleic Acid
428 Polymerase. *J. Biol. Chem.*, 244, 6168–6176.
- 429 15. Murakami, K., Kimura, M., Owens, J.T., Meares, C.F. and Ishihama, A. (1997) The two subunits of
430 *Escherichia coli* RNA polymerase are asymmetrically arranged and contact different halves of the
431 DNA upstream element. *Proc. Natl. Acad. Sci.*, 94, 1709–1714.
- 432 16. Bedwell, D., Davis, G., Gosink, M., Post, L., Nomura, M., Kestler, H., Zengel, J.M. and Lindahl, L.
433 (1985) Nucleotide sequence of the alpha ribosomal protein operon of *Escherichia coli*. *Nucleic Acids*
434 *Res.*, 13, 3891–3902.
- 435 17. Thomas, M.S., Bedwell, D.M. and Nomura, M. (1987) Regulation of α operon gene expression in
436 *Escherichia coli*. *J. Mol. Biol.*, 196, 333–345.
- 437 18. Sutherland, C. and Murakami, K.S. (2018) An Introduction to the Structure and Function of the
438 Catalytic Core Enzyme of *Escherichia coli* RNA Polymerase. *EcoSal Plus*, 8, ecosalplus.ESP-0004-
439 2018.
- 440 19. Koonin, E. V., Krupovic, M., Ishino, S. and Ishino, Y. The replication machinery of LUCA: common
441 origin of DNA replication and transcription. 10.1186/s12915-020-00800-9.
- 442 20. Zakharova, N., Paster, B.J., Wesley, I., Dewhirst, F.E., Berg, D.E. and Severinov, K. V. (1999)
443 Fused and overlapping *rpoB* and *rpoC* genes in helicobacters, campylobacters, and related bacteria.
444 *J. Bacteriol.*, 181, 3857–3859.
- 445 21. Severinov, K., Mooney, R., Darst, S.A. and Landick, R. (1997) Tethering of the Large Subunits of
446 *Escherichia coli* RNA Polymerase. *J. Biol. Chem.*, 272, 24137–24140.
- 447 22. Ralling, G. and Linn, T. (1984) Relative activities of the transcriptional regulatory sites in the
448 *rplKALrpoBC* gene cluster of *Escherichia coli*. *J. Bacteriol.*, 158, 279–285.
- 449 23. Burgess, R.R. (1971) RNA POLYMERASE. *Annu. Rev. Biochem.*, 40, 711–740.
- 450 24. Whitby, M.C., Vincent, S.D. and Lloyd, R.G. (1994) Branch migration of Holliday junctions:
451 identification of RecG protein as a junction specific DNA helicase. *EMBO J.*, 13, 5220–5228.
- 452 25. Persson, B. (1997) The *spoU* gene of *Escherichia coli*, the fourth gene of the *spoT* operon, is
453 essential for tRNA (Gm18) 2'-O-methyltransferase activity. *Nucleic Acids Res.*, 25, 4093–4097.
- 454 26. Chatterji, D. and Kumar Ojha, A. (2001) Revisiting the stringent response, ppGpp and starvation
455 signaling. *Curr. Opin. Microbiol.*, 4, 160–165.

- 456 27. CASHEL, M. and GALLANT, J. (1969) Two Compounds implicated in the Function of the RC
457 Gene of *Escherichia coli*. *Nature*, 221, 838–841.
- 458 28. Durfee, T., Hansen, A.-M., Zhi, H., Blattner, F.R. and Jin, D.J. (2008) Transcription Profiling of the
459 Stringent Response in *Escherichia coli*. *J. Bacteriol.*, 190, 1084–1096.
- 460 29. Srivatsan, A. and Wang, J.D. (2008) Control of bacterial transcription, translation and replication
461 by (p)ppGpp. *Curr. Opin. Microbiol.*, 11, 100–105.
- 462 30. Igarashi, K., Fujita, N. and Ishihama, A. (1989) Promoter selectivity of *Escherichia coli* RNA
463 polymerase: omega factor is responsible for the ppGpp sensitivity. *Nucleic Acids Res.*, 17, 8755–8765.
- 464 31. Mukherjee, K., Nagai, H., Shimamoto, N. and Chatterji, D. (1999) GroEL is involved in activation of
465 *Escherichia coli* RNA polymerase devoid of the omega subunit in vivo. *Eur. J. Biochem.*, 266, 228–
466 235.
- 467 32. Gruber, T.M. and Gross, C.A. (2003) Multiple Sigma Subunits and the Partitioning of Bacterial
468 Transcription Space. *Annu. Rev. Microbiol.*, 57, 441–466.
- 469 33. Tripathi, L., Zhang, Y. and Lin, Z. (2014) Bacterial Sigma Factors as Targets for Engineered or
470 Synthetic Transcriptional Control. *Front. Bioeng. Biotechnol.*, 2, 33.
- 471 34. Werner, F. and Grohmann, D. (2011) Evolution of multisubunit RNA polymerases in the three
472 domains of life. *Nat. Rev. Microbiol.*, 9, 85–98.
- 473 35. Albert, H., Dale, E.C., Lee, E. and Ow, D.W. (1995) Site-specific integration of DNA into wild-type
474 and mutant *lox* sites placed in the plant genome. *Plant J.*, 7, 649–659.
- 475 36. Deatherage, D.E. and Barrick, J.E. (2014) Identification of Mutations in Laboratory-Evolved
476 Microbes from Next-Generation Sequencing Data Using breseq. In *Methods in molecular biology*
477 (Clifton, N.J.). NIH Public Access, Vol. 1151, pp. 165–188.
- 478 37. Wenk, S., Yishai, O., Lindner, S.N. and Bar-Even, A. (2018) An Engineering Approach for Rewiring
479 Microbial Metabolism. In *Methods in Enzymology*. Academic Press, Vol. 608, pp. 329–367.
- 480 38. Bonde, M.T., Pedersen, M., Klausen, M.S., Jensen, S.I., Wulff, T., Harrison, S., Nielsen, A.T.,
481 Herrgård, M.J. and Sommer, M.O.A. (2016) Predictable tuning of protein expression in bacteria. *Nat.*
482 *Methods*, 13, 233–236.
- 483 39. Wang, K., Boysen, C., Shizuya, H., Simon, M.I. and Hood, L. (1997) Complete Nucleotide
484 Sequence of Two Generations of a Bacterial Artificial Chromosome Cloning Vector. *Biotechniques*, 23,
485 992–994.
- 486 40. Mülleder, M., Capuano, F., Pir, P., Christen, S., Sauer, U., Oliver, S.G. and Ralser, M. (2012) A
487 prototrophic deletion mutant collection for yeast metabolomics and systems biology. *Nat. Biotechnol.*,
488 30, 1176–1178.
- 489 41. Creutzburg, S.C.A. (2020) Structure-function relations of RNA molecules involved in gene
490 expression and host defence. 10.18174/532325.
- 491 42. Choe, D., Lee, J.H., Yoo, M., Hwang, S., Sung, B.H., Cho, S., Palsson, B., Kim, S.C. and Cho, B.-K.
492 (2019) Adaptive laboratory evolution of a genome-reduced *Escherichia coli*. *Nat. Commun.*, 10, 935.
- 493 43. Tenaille, O., Rodríguez-Verdugo, A., Gaut, R.L., McDonald, P., Bennett, A.F., Long, A.D. and
494 Gaut, B.S. (2012) The Molecular Diversity of Adaptive Convergence. *Science (80-.)*, 335, 457–461.

- 495 44. Du,B., Olson,C.A., Sastry,A. V., Fang,X., Phaneuf,P. V., Chen,K., Wu,M., Szubin,R., Xu,S.,
496 Gao,Y., et al. (2020) Adaptive laboratory evolution of *Escherichia coli* under acid stress. *Microbiology*,
497 166, 141–148.
- 498 45. Mohamed,E.T., Mundhada,H., Landberg,J., Cann,I., Mackie,R.I., Nielsen,A.T., Herrgård,M.J.
499 and Feist,A.M. (2019) Generation of an *E. coli* platform strain for improved sucrose utilization using
500 adaptive laboratory evolution. *Microb. Cell Fact.*, 18, 116.
- 501 46. Conrad,T.M., Frazier,M., Joyce,A.R., Cho,B.K., Knight,E.M., Lewis,N.E., Landick,R. and
502 Palsson,B. (2010) RNA polymerase mutants found through adaptive evolution reprogram *Escherichia*
503 *coli* for optimal growth in minimal media. *Proc. Natl. Acad. Sci. U. S. A.*, 107, 20500–20505.
- 504 47. Murphy,H. and Cashel,M. (2003) Isolation of RNA Polymerase Suppressors of a (p)ppGpp
505 Deficiency. In *Methods in Enzymology*. Academic Press Inc., Vol. 371, pp. 596–601.
- 506 48. Klein-Marcuschamer,D., Santos,C.N.S., Yu,H. and Stephanopoulos,G. (2009) Mutagenesis of
507 the Bacterial RNA Polymerase Alpha Subunit for Improvement of Complex Phenotypes. *Appl. Environ.*
508 *Microbiol.*, 75, 2705–2711.
- 509 49. Conrad,T.M., Lewis,N.E. and Palsson,B.Ø. (2011) Microbial laboratory evolution in the era of
510 genome-scale science. *Mol. Syst. Biol.*, 7, 509.
- 511 50. Phaneuf,P. V, Gosting,D., Palsson,B.O. and Feist,A.M. (2019) ALEdb 1.0: a database of
512 mutations from adaptive laboratory evolution experimentation. *Nucleic Acids Res.*, 47, D1164–D1171.
- 513 51. Cheng,K.K., Lee,B.S., Masuda,T., Ito,T., Ikeda,K., Hirayama,A., Deng,L., Dong,J., Shimizu,K.,
514 Soga,T., et al. (2014) Global metabolic network reorganization by adaptive mutations allows fast
515 growth of *Escherichia coli* on glycerol. *Nat. Commun.*, 5, 1–9.
- 516 52. Dragosits,M., Mozhayskiy,V., Quinones-Soto,S., Park,J. and Tagkopoulos,I. (2013) Evolutionary
517 potential, cross-stress behavior and the genetic basis of acquired stress resistance in *Escherichia coli*.
518 *Mol. Syst. Biol.*, 9, 643.
- 519 53. Utrilla,J., O'Brien,E.J., Chen,K., McCloskey,D., Cheung,J., Wang,H., Armenta-Medina,D.,
520 Feist,A.M. and Palsson,B.O. (2016) Global Rebalancing of Cellular Resources by Pleiotropic Point
521 Mutations Illustrates a Multi-scale Mechanism of Adaptive Evolution. *Cell Syst.*, 2, 260–271.
- 522 54. Saecker,R.M., Record,M.T. and DeHaseth,P.L. (2011) Mechanism of Bacterial Transcription
523 Initiation: RNA Polymerase - Promoter Binding, Isomerization to Initiation-Competent Open
524 Complexes, and Initiation of RNA Synthesis. *J. Mol. Biol.*, 412, 754–771.
- 525 55. Hutchison,C.A., Chuang,R.-Y., Noskov,V.N., Assad-Garcia,N., Deerinck,T.J., Ellisman,M.H.,
526 Gill,J., Kannan,K., Karas,B.J., Ma,L., et al. (2016) Design and synthesis of a minimal bacterial
527 genome. *Science (80-)*, 351.
- 528 56. Kuijpers,N.G.A., Solis-Escalante,D., Luttik,M.A.H., Bisschops,M.M.M., Boonekamp,F.J., van den
529 Broek,M., Pronk,J.T., Daran,J.-M. and Daran-Lapujade,P. (2016) Pathway swapping: Toward modular
530 engineering of essential cellular processes. *Proc. Natl. Acad. Sci.*, 113, 15060–15065.
- 531
532
533
534